

# Phthalate Esters Released from Plastics Promote Biofilm Formation and Chlorine Resistance

Haibo Wang, Pingfeng Yu,\* Cory Schwarz, Bo Zhang, Lixin Huo, Baoyou Shi, and Pedro J. J. Alvarez\*



Cite This: *Environ. Sci. Technol.* 2022, 56, 1081–1090



Read Online

ACCESS |



Metrics & More



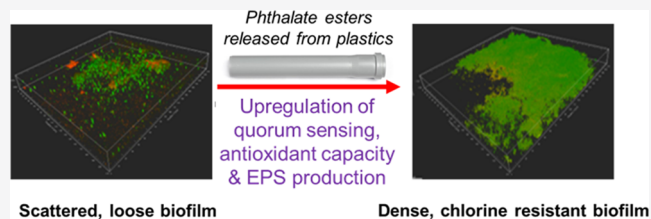
Article Recommendations



Supporting Information

**ABSTRACT:** Phthalate esters (PAEs) are commonly released from plastic pipes in some water distribution systems. Here, we show that exposure to a low concentration (1–10  $\mu\text{g/L}$ ) of three PAEs (dimethyl phthalate (DMP), di-n-hexyl phthalate (DnHP), and di-(2-ethylhexyl) phthalate (DEHP)) promotes *Pseudomonas* biofilm formation and resistance to free chlorine. At PAE concentrations ranging from 1 to 5  $\mu\text{g/L}$ , genes coding for quorum sensing, extracellular polymeric substances excretion, and oxidative stress resistance were upregulated by 2.7- to 16.8-fold, 2.1- to 18.9-fold, and 1.6- to 9.9-fold, respectively. Accordingly, more biofilm matrix was produced and the polysaccharide and eDNA contents increased by 30.3–82.3 and 10.3–39.3%, respectively, relative to the unexposed controls. Confocal laser scanning microscopy showed that PAE exposure stimulated biofilm densification (volumetric fraction increased from 27.1 to 38.0–50.6%), which would hinder disinfectant diffusion. Biofilm densification was verified by atomic force microscopy, which measured an increase of elastic modulus by 2.0- to 3.2-fold. PAE exposure also stimulated the antioxidative system, with cell-normalized superoxide dismutase, catalase, and glutathione activities increasing by 1.8- to 3.0-fold, 1.0- to 2.0-fold, and 1.2- to 1.6-fold, respectively. This likely protected cells against oxidative damage by chlorine. Overall, we demonstrate that biofilm exposure to environmentally relevant levels of PAEs can upregulate molecular processes and physiologic changes that promote biofilm densification and antioxidative system expression, which enhance biofilm resistance to disinfectants.

**KEYWORDS:** phthalate esters, oxidative stress, biofilm densification, disinfectant resistance



## INTRODUCTION

Biofilms are the predominant form of microbes living in drinking water distribution systems (DWDS).<sup>1</sup> As surface-attached microbial aggregates surrounded by excreted extracellular polymeric substances (EPS), biofilms can shelter pathogens and antimicrobial-resistant bacteria from common disinfectants such as free residual chlorine.<sup>2,3</sup> The relatively stable biofilm microenvironment can also facilitate horizontal gene transfer and accelerate the development of bacterial resistance to disinfectants.<sup>2,3</sup> Moreover, biofilms are closely correlated with biofouling and biocorrosion that contribute significantly to infrastructure degradation and water quality deterioration.<sup>4–6</sup> Therefore, it is crucial to advance our understanding of factors that shape DWDS biofilm structure and affect their susceptibility to disinfectants.

DWDS biofilm assembly is primarily controlled by water characteristics (including the presence of residual or infiltrated substrates and nutrients), pipeline materials, and operational conditions.<sup>7,8</sup> Plastic water distribution pipes and some water storage tanks, such as those made of high-density polyethylene (HDPE) and poly(vinyl chloride) (PVC), are extensively used due to their flexibility and low cost.<sup>9</sup> Notably, these materials contain plasticizers such as phthalate esters (PAEs), which may leach during plastic aging since PAEs are not covalently bound

to the polymers.<sup>10,11</sup> The release of PAEs from plastics can exceed 2 g/kg depending on the thickness, aging status, and composition of the plastics.<sup>12</sup> Moreover, plastic debris (e.g., microplastics) and the associated PAEs have been frequently detected in aquatic environments, including drinking water sources.<sup>13,14</sup> The total concentration of dissolved plus sorbed PAEs can reach 2 mg/L in surface water.<sup>15,16</sup> The presence of phthalates in drinking water samples has also been reported worldwide with total PAE concentrations ranging from 0.1 to 10  $\mu\text{g/L}$ ,<sup>16,17</sup> which indicates that PAEs cannot be removed effectively by conventional water treatment processes. Therefore, it is important to investigate the influence of incidentally introduced or *in situ* generated PAEs on the formation and resistance of DWDS biofilms.

Several studies have addressed the effects of PAEs on microbial community structure and function besides their well-known endocrine-disrupting potential in eukaryotic organ-

Received: July 19, 2021

Revised: December 10, 2021

Accepted: December 29, 2021

Published: January 7, 2022



isms.<sup>18–20</sup> Exposure to high levels (i.e., 20–40 mg/L) of dimethyl phthalate (DMP) significantly inhibited planktonic bacterial activity because of cell permeability disruption and intracellular reactive oxygen species (ROS) induction.<sup>21</sup> However, DMP at 20 mg/L upregulated genes for carbohydrate transport, metabolism, and energy production in a soil microbiome.<sup>22</sup> Furthermore, di-(2-ethylhexyl) phthalate (DEHP) at 1 mg/L altered a periphytic biofilm microbial community but not its metabolic functions.<sup>23</sup> Recent studies found that plastic-attached microorganisms were metabolically more active than those in the surrounding water, possibly due to exposure to plasticizers.<sup>24</sup> These studies show that PAEs with different structures and at different concentrations may elicit various microbial responses. However, it is unknown how PAEs at environmentally relevant levels affect biofilm development and resistance to disinfection, which is important to inform microbial risk assessment as well as plasticizer choices for plastic pipelines and water storage tanks.

In this study, we investigate the dose–response behavior of biofilm to three different PAEs (i.e., DMP, di-n-hexyl phthalate (DnHP) and DEHP). DMP, DnHP, and DEHP are commonly used as plasticizers while DMP is the main PAE released from PVC materials,<sup>25,26</sup> all of which have been detected in tap water.<sup>16,17,27</sup> *Pseudomonas aeruginosa* was chosen as the model strain for biofilm study due to its common occurrence in biofilms found in various environments,<sup>28,29</sup> including water distribution and storage systems.<sup>1,30</sup> Biofilm biomass and disinfectant resistance were monitored after exposure to these PAEs at DWDS-relevant levels ranging from 1 to 10  $\mu\text{g/L}$ .<sup>15,17</sup> Microbial enzymatic activity and biofilm EPS content (i.e., polysaccharides, proteins, and eDNA) were examined to gain insights into enhanced biofilm disinfectant resistance after PAE exposure. Biofilm integrity and density were measured via confocal laser scanning microscopy (CLSM) and atomic force microscope (AFM) to corroborate enhanced biofilm resistance to chlorine. We also analyzed the transcriptional response of biofilm-related (i.e., quorum sensing production and EPS excretion) and antioxidative system genes. Multispecies biofilms of DWDS-sourced microbes were also cultured under continuous flow conditions in the presence and absence of selected PAEs to inform the effects of PAEs on realistic biofilm resiliency.

## MATERIALS AND METHODS

**Bacterial Strain, Culture Conditions, and Reagents.** *P. aeruginosa* PAO1 (ATCC 15629) was used for experiments involving pure biofilms. This bacterial strain was grown in Davis Minimal Nutrient Broth (DMNB, BD, Sparks, MD), which contained 7 g/L  $\text{KH}_2\text{PO}_4$ , 2 g/L  $\text{K}_2\text{HPO}_4$ , 0.5 g/L sodium citrate, 0.1 g/L  $\text{MgSO}_4$ , 1 g/L  $(\text{NH}_4)_2\text{SO}_4$ , and 5.0 g/L glucose. Pure and mixed biofilm assembly experiments were also performed in DMNB and supplemented with different concentrations of the three examined PAEs (added separately). *P. aeruginosa* was grown on DMNB, harvested during exponential growth, and enumerated via colony assay on *Pseudomonas* selective agar (BD, Sparks, MD) by counting colony-forming units (CFU).

Reagents purchased from Invitrogen (Grand Island, NY) include RNaseOUT, Random primers, dNTP set, Superscript II reverse transcriptase, and propidium iodide. Costar 12- or 96-well plates and cell scrapers were bought from Corning, Inc. (Corning, NY). RNA protective reagent, QIA quick PCR Purification Kit, and RNeasy Mini Kit were obtained from

Qiagen Inc. (Valencia, CA). DMP, DnHP, and DEHP were purchased from EMD Millipore, Inc. (Darmstadt Germany), with their physical–chemical characteristics shown in Table S1. ROS assay kit, superoxide dismutase (SOD) assay kit, catalase (CAT) assay kit, and glutathione (GSH) assay kit were obtained from Nanjing Jiancheng Bioengineering Institute, China.

**Biofilm Formation Under Exposure to Different PAE Concentrations.** *P. aeruginosa* (10  $\mu\text{L}$ , optical density at 600 nm of 0.1) was inoculated into 190  $\mu\text{L}$  of fresh DMNB in Greiner Bio-One SCREENSTAR 96-well microtiter plates (Monroe, NC). The microplates were incubated at 25 °C with horizontal shaking at 60 rpm to promote biofilm attachment and development. After 24 h, the suspension was removed and each well was washed gently with phosphate-buffered saline (PBS) to ensure removal of unattached cells. Subsequently, 200  $\mu\text{L}$  of DMNB amended with DMP, DnHP, or DEHP at a final concentration of 1, 2, 5, or 10  $\mu\text{g/L}$  was added into individual wells. Each condition was performed in triplicate, with DMNB amended with PBS used as the untreated control. The liquid culture under each condition was replaced with fresh amended medium every 8 h. After 24 h PAE exposure (i.e., three replacements with fresh amended medium), the wells were washed twice with PBS to remove unbound cells and the attached biofilm was characterized as follows.

**Biofilm Biomass Quantification and Disinfection Resistance Characterization.** The biofilm biomass was estimated by crystal violet assay (at an optical density of 595 nm) as previously reported.<sup>31</sup> Biofilm hydrophobicity was measured via a water contact angle assay using a contact angle meter (OCA 1SEC, Germany).<sup>32</sup> To test biofilm disinfectant resistance, the above biofilms were exposed to 2 mg/L sodium hypochlorite (free chlorine) in PBS at 25 °C for 4 h. The disinfection efficiency was calculated as the relative changes in overall biofilm biomass before and after treatment.<sup>3</sup> For viable bacteria enumeration, the attached biofilm was dispersed as follows. Briefly, 100  $\mu\text{L}$  of 0.5% Tween-20 in PBS was added to each well, sonicated at 40 kHz for 5 min in a 4 °C bath sonicator (Branson, Danbury, CT), and then the suspension was subject to colony assay. Biofilm EPS were obtained by 2% (w/v) EDTA (disodium salt) extracting solution and analyzed in terms of protein, polysaccharide, and extracellular DNA (eDNA) using bovine serum, D-glucose, and Calf Thymus DNA, respectively, as the standards.<sup>3,33</sup> The details of extraction procedures and analysis (including standard curves) are shown in Supporting Information (Text S1).

Biofilm adenosine triphosphate (ATP) was analyzed by Bioluminescent Assay Kit (Sigma, CA) in a Modulus Single tube multimode reader (Promega Biosystems Sunnyvale, Inc., CA) to determine the biofilm activity after 24 h PAE exposure.<sup>34</sup> For ROS measurements, the cells were incubated with 20  $\mu\text{M}$  DCFH-DA solution in the dark for 30 min.<sup>36</sup> Then, the cells were rinsed with PBS (0.1M, pH = 7.4) and seeded in black 96-well plates containing different PAEs. After incubating for 6 h, the green fluorescence (oxidized DCFH-DA) was quantified using a Multimode Plate Reader (PerkinElmer). The excitation and emission wavelengths were set at 488 and 525 nm, respectively. In addition, the ROS scavenger N-acetyl-L-cysteine with a final concentration of 100  $\mu\text{M}$  was added to PAE-exposed bacterial cells to verify the role of oxidative stress in the biofilm stimulation. The differences in oxidative stress response to the PAE treatments were also detected by the antioxidative system analysis.

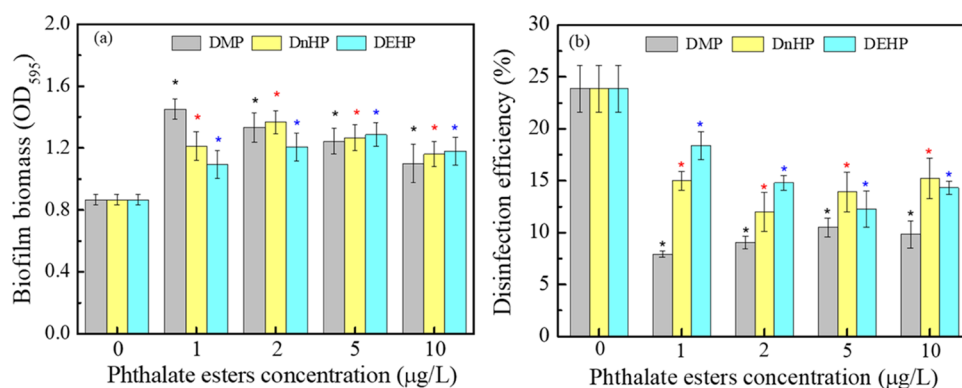


**Figure 1.** Increase in *Pseudomonas* biofilm biomass (grown on DMNB medium) and disinfectant resistance when exposed to different concentrations of PAEs. Biofilms exposed to PAEs (DMP, DnHP, and DEHP) for 24 h produced more biofilm matrix (a) and displayed enhanced resistance to sodium hypochlorite disinfection (b). Biomass was measured using the crystal violet stain assay. Error bars represent  $\pm$  one standard deviation from the mean of independent triplicates. Asterisks (\*) represent differences ( $p < 0.05$ ) between treatment and unexposed control, based on Student's *t*-test.

Specifically, SOD activity, CAT activity, and GSH concentration were determined by spectrometry assays using the SOD assay kit, CAT assay kit, and GSH assay kit following the manufacturer's instructions. The details for ROS and antioxidative system analysis are shown in the Supporting Information (Texts S2 and S3).

#### Biofilm Structure Analyses with CLSM and AFM.

Biofilm structure was characterized by confocal laser scanning microscopy (CLSM) (Nikon, Tokyo, Japan) as previously reported.<sup>35</sup> Briefly, PBS rinsed biofilms were fixed with 2.5% glutaraldehyde solution and stained with BacLight LIVE/DEAD Staining kit (Molecular Probes, Inc.). The CLSM images of live and dead cells were obtained using a 488 nm laser for excitation of SYTO 9 (green) and 560 nm laser for excitation of propidium iodide (PI, red), respectively. Z-stack images were collected and rendered into three-dimensional (3D) images to visualize the structure of biofilm using Nikon NIS-Element software (Nikon, Tokyo, Japan). For each biofilm sample, three positions were selected for image acquisition and further biofilm analysis in terms of biofilm coverage, live/dead cell ratios, and bacterial volumetric fractions performed in the NIS-Element software. Bacterial volumetric fraction was calculated as the ratio of total cell volume to total biofilm volume.

The biofilm surface morphology<sup>37</sup> and elastic modulus (Young's modulus,  $E$ )<sup>38</sup> were obtained by AFM in a dry environment.<sup>39</sup> Briefly, following the AFM probe calibration, indentation measurements were repeated at seven randomly selected locations in each deposit sample with the test area size set to  $50 \times 50 \mu\text{m}$ . At each location, the indentation tests were repeated 10 times. In total, 70 indentation tests were conducted on each deposit sample through the force volume model of AFM. The force-indent depth curves of 70 points of each sample were obtained. The biofilm roughness was determined from the 3D AFM images of biofilm surface morphology using NanoScope Analysis software (Version 1.80) with default parameters.<sup>40</sup> The elastic modulus ( $E$ ) was obtained by fitting force-indent depth curves via the Snedden model in the NanoScope Analysis software (Version 1.80). All of the measured values of Young's modulus ( $E$ ) were divided into four groups: a soft group with  $E < 10000 \text{ MPa}$ , a middle hardness group with  $10000 \text{ MPa} < E < 30000 \text{ MPa}$ , a hard group with  $30000 \text{ MPa} < E < 50000 \text{ MPa}$ , and a very hard group with  $E > 50000 \text{ MPa}$ .<sup>38,41</sup>

#### Differential Gene Expression Analysis (RNA-seq and RT-qPCR).

Expression of biofilm formation genes generally outpaces EPS secretion and biofilm densification,<sup>3,42</sup> so biofilms were sampled for transcriptomic analysis before physicochemical characterization, following 6 h of exposure to PAEs at different concentrations. The transcriptomic analysis included biofilm-related genes (i.e., *lasI*, *lasR*, *rhlI*, and *rhlR* for quorum sensing; *sagS* for bacterial adherence; *pslA* and *pelA* for EPS excretion)<sup>43</sup> and genes involved in antioxidative systems (i.e., *sodM* and *msrB* for reductases).<sup>44</sup> The 16S RNA gene with relatively stable expression levels in biofilm bacteria was used as a reference gene for gene expression normalization. The primers for these genes are shown in Table S2. Total RNA was extracted from biofilm samples using the RNeasy Mini Kit (Invitrogen, Thermo Fisher Scientific) and subject to DNase treatment for residual DNA removal. After heat-inactivation of enzymes, the purified RNA was converted into cDNA and quantified with qPCR as previously reported. The  $2^{-\Delta\Delta\text{CT}}$  method was used to quantify differential gene expression relative to the reference gene as detailed in Text S4 in the Supporting Information, and the heatmap was generated in the R platform (R version 3.2.2; [www.rproject.org](http://www.rproject.org)) to show the changes in expression of targeted genes in the exposed groups relative to the control group without PAE exposure.

#### Multispecies Biofilm Cultivation and Exposure Tests.

Multispecies biofilms were established on concrete coupons (BioSurface Technology, Montana) in standard CDC biofilm reactors at 25 °C with magnetic stirring at 60 rpm. Microbial samples from a drinking water pipe at Rice University were inoculated into the biofilm reactors continuously fed with DMNB at 100 mL/h. After 1-week biofilm formation, two reactors were fed with DMNB amended with 1 µg/L DMP or 5 µg/L DEHP, while the control reactor continued to receive plain DMNB. Each day, three coupons were sampled from each reactor for biofilm mass measurement using the crystal violet optical assay. After 7 days, the biofilm-attached coupons were sampled for biofilm structure analysis via CLSM, bacterial quantification via plate assay, biofilm EPS quantification via colorimetric methods, and disinfectant resistance tests described above.

**Statistical Analyses.** All of the experiments were performed independently at least in triplicate. ANOVA and



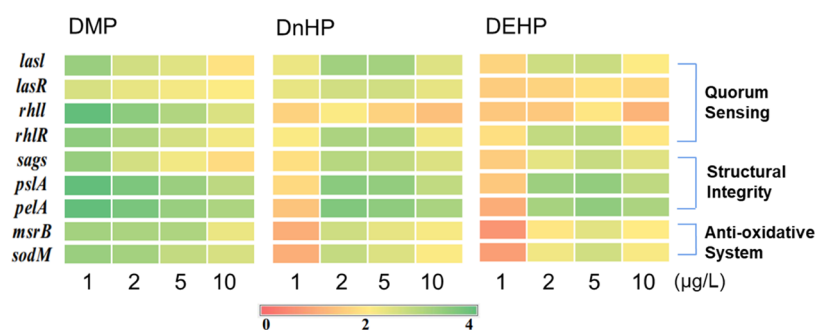


**Figure 2.** Upregulation of genes associated with *Pseudomonas* biofilm formation and resistance after exposure to different concentrations of PAEs. RT-qPCR was performed targeting genes associated with quorum sensing, structural integrity, and bacterial antioxidative systems. The quantification of each gene was expressed as the fold change (fold changes are log<sub>2</sub> transformed) relative to unexposed controls. Results are the mean of independent triplicates.

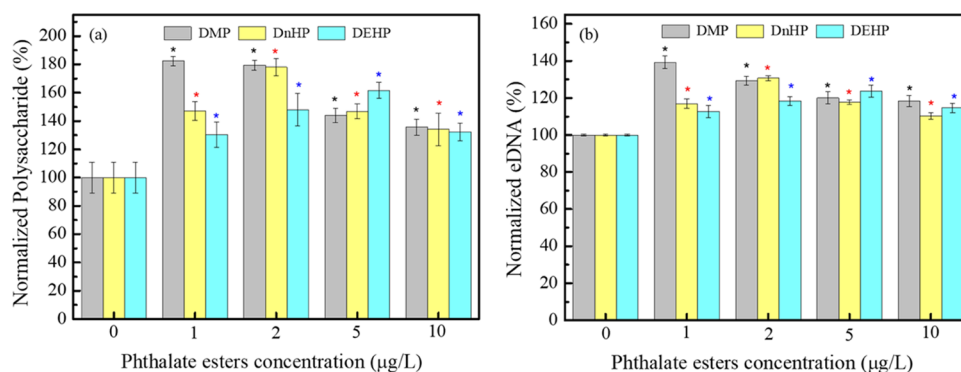


**Figure 3.** Production of EPS in *Pseudomonas* biofilm after exposure to different concentrations of PAEs. (a) Total polysaccharide content was analyzed using the phenol-sulfuric acid colorimetric method and normalized per live cell and (b) the eDNA content was quantified with the diphenylamine reagent method and normalized per live cell. These components were further normalized by those in the group without PAEs addition. Asterisks (\*) represent differences ( $p < 0.05$ ) between treatment and unexposed control, based on Student's  $t$ -test. Error bars represent  $\pm$  one standard deviation from the mean of at least three independent replicates.

Student's  $t$ -test with Bonferroni correction for multiple comparisons were used to determine statistical significance.

## RESULTS AND DISCUSSION

**Low Levels of PAEs Promoted *Pseudomonas* Biofilm Formation.** *Pseudomonas* biofilm exposure to three PAEs (DMP, DnHP, and DEHP) at concentrations ranging from 1 to 10  $\mu\text{g/L}$  (which are insufficient to support significant cell growth, Figure S1) stimulated biofilm formation and biomass growth to different degrees (Figure 1a). The DMNB medium contained citrate (500 mg/L) and glucose (5.0 g/L) as the main carbon source. DMP, the lowest-molecular-weight PAE considered, showed the highest stimulation at 1  $\mu\text{g/L}$  with biomass increasing by 67.5% ( $p < 0.01$ ). As the DMP concentration increased, the stimulatory effect on the biofilm decreased (Figure 1a), perhaps due to a previously reported inhibitory effect of DMP on bacterial activity.<sup>45,46</sup> DnHP and DEHP, the higher-molecular-weight PAEs with higher hydrophobicity and lower solubility (Table S1), exhibited the highest stimulation at 2 and 5  $\mu\text{g/L}$ , respectively. The corresponding biomass increased by 54.2% for DnHP and 42.7% for DEHP relative to the unexposed control ( $p < 0.01$ ). Based on statistical analysis (Table S3), 1  $\mu\text{g/L}$  DMP and 2  $\mu\text{g/L}$  DnHP are the “peak-effect” concentrations for biofilm stimulation. Although 5  $\mu\text{g/L}$  DEHP was not significantly more stimulative than 2 or 10  $\mu\text{g/L}$  DEHP, it was significantly more stimulative than 1  $\mu\text{g/L}$  DEHP. Therefore, we used these three conditions for detailed biofilm characterization and

discussion. The different peak-effect concentrations for the three PAEs might be due to differences in their physicochemical properties (Table S1) that affect their bioavailability and bacterial toxicity.<sup>20</sup>

Consistently, biofilm bacteria density increased from  $1.0 \times 10^8$  to  $1.6 \times 10^8$ ,  $1.3 \times 10^8$ , and  $1.2 \times 10^8$  CFU/cm<sup>2</sup> after exposure to the peak-effect concentrations of DMP, DnHP, and DEHP, respectively (Figure S2). Moreover, ATP activity measurements showed that exposure to low PAE levels increased the activity of biofilm-dwelling bacteria (Figure S3). DMP, DnHP, and DEHP at peak-effect concentrations induced an increase in cellular ATP from  $1.6 \times 10^{-10}$  to  $6.6 \times 10^{-10}$ ,  $5.2 \times 10^{-10}$ , and  $4.6 \times 10^{-10}$  nmol/CFU, respectively. Biofilm growth promotion was positively correlated with resistance to disinfection ( $R = 0.99$ ,  $p < 0.01$ ). Specifically, biofilms without PAE exposure experienced a decrease in biomass of about 24% after free chlorine treatment (2 mg/L sodium hypochlorite), while the biofilms exposed to 1  $\mu\text{g/L}$  DMP, 2  $\mu\text{g/L}$  DnHP, and 5  $\mu\text{g/L}$  DEHP had lower biomass decreases of only 8, 12, and 12%, respectively (Figure 1b).

**Low Levels of PAEs Upregulated QS Generation and EPS Excretion.** To protect bacteria from detrimental chemicals, biofilms can sometimes respond to sublethal levels of antimicrobial agents with enhanced microbial communication, resource allocation efficiency, and EPS generation, which can confer biofilm resistance to multiple environmental stressors.<sup>47,48</sup> Transcriptomic analysis revealed that genes associated with QS and EPS excretion were significantly

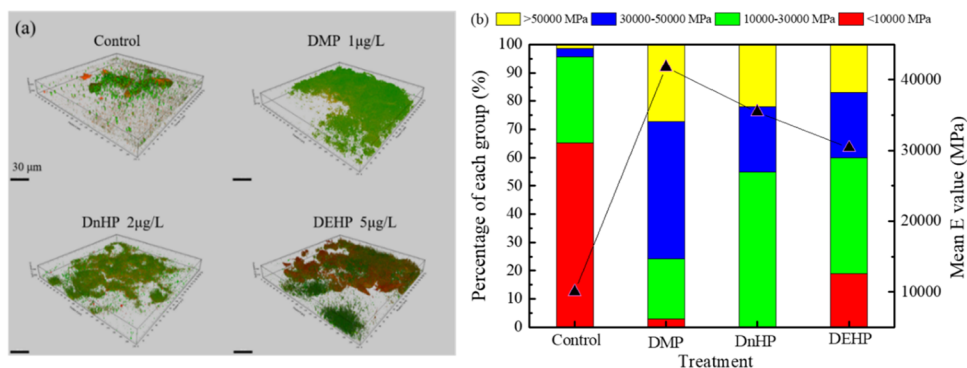


**Figure 4.** Low levels of PAE exposure modified *Pseudomonas* biofilm structure and resilience. (a) Confocal laser scanning microscopy (CLSM) images showed *Pseudomonas* biofilm densification after exposure to different concentrations of PAEs. The biofilm was stained with SYTO 9 and propidium iodide (PI) from LIVE/DEAD BacLight kit. The green and red colors represent the lived and dead cells, respectively. Scale bar represents 30  $\mu\text{m}$ . (b) Percentage stacked bar for the Young modulus ( $E$ ) of the biofilm after exposure to different concentrations of PAEs (DMP 1  $\mu\text{g/L}$ , DnHP 2  $\mu\text{g/L}$ , and DEHP 5  $\mu\text{g/L}$ ). The black line shows the mean  $E$  value in three representative biofilm sections after different treatments.

upregulated after exposure to the tested PAEs for 6 h (Figure 2). Specifically, four genes regulating *P. aeruginosa* QS secretion (i.e., *lasI* and *lasR* in the *las* QS system, and *rhlI* and *rhlR* in the *rhl* QS system) were upregulated by 5.7- to 16.8-fold upon exposure to 1  $\mu\text{g/L}$  DMP relative to control groups. Accordingly, gene *sagS* regulating bacterial adherence was also upregulated by 10.1-fold, and genes *pslA* and *pelA* associated with LPS biosynthesis and EPS excretion were upregulated by 16.9- and 18.9-fold upon exposure to 1  $\mu\text{g/L}$  DMP relative to control groups without PAEs exposure, respectively. Consistently, the amount of polysaccharide, eDNA, and protein increased significantly by  $82.3 \pm 3.4$ ,  $39.3 \pm 3.4$ , and  $14.0 \pm 1.6\%$  per live cell, respectively, relative to control groups in 24 h (Figures 3 and S4).

Similarly, 2  $\mu\text{g/L}$  DnHP and 5  $\mu\text{g/L}$  DEHP upregulated these genes. QS secretion genes were upregulated by 4.2- to 9.3-fold upon exposure to 2  $\mu\text{g/L}$  DnHP and 3.6- to 7.5-fold upon exposure to 5  $\mu\text{g/L}$  DEHP relative to control groups (Figure 2). For the biofilms exposed to 2  $\mu\text{g/L}$  DnHP, the amount of polysaccharide, eDNA and protein increased significantly by  $78.0 \pm 6.2$ ,  $30.7 \pm 1.3$ , and  $9.3 \pm 1.5\%$  per live cell, respectively, relative to control groups (Figures 3 and S4). The corresponding relative amount of polysaccharide, eDNA, and protein increased by  $61.7 \pm 5.7$ ,  $23.7 \pm 3.3$ , and  $7.7 \pm 0.5\%$  for the biofilms exposed to 5  $\mu\text{g/L}$  DEHP.

The trends in gene expression were positively correlated with biofilm EPS excretion and resultant disinfectant resistance for the three tested PAEs (Figures 1–3). Polysaccharides with high viscosity can directly adsorb PAEs and increase cross-linking within the biofilm by interacting with themselves or other heterologous molecules.<sup>3,49</sup> Moreover, eDNA can function as an intercellular connector through hydrogen bonding and electrostatic interactions, which helps maintain biofilm structural integrity.<sup>50</sup> Proteins can hinder disinfectant penetration by reacting with disinfectant and reducing disinfectant concentration within biofilms.<sup>51</sup> Therefore, enhanced EPS excretion generally improves resistance to disinfectants by hindering the transport of disinfectants into the biofilm matrix.<sup>52</sup>

**Low Levels of PAEs Modified Biofilm Structure and Increased Biofilm Resilience.** CLSM imaging corroborated enhanced biofilm integrity after exposure to low levels of PAEs. The control biofilm was scattered with a volumetric fraction of 27.1% (Figure 4a). When the biofilms were exposed to the

peak-effect concentrations of DMP (i.e., 1  $\mu\text{g/L}$ ), DnHP (i.e., 2  $\mu\text{g/L}$ ), and DEHP (i.e., 5  $\mu\text{g/L}$ ), the biofilm bacterial volumetric fraction increased to 50.6, 38.9, and 38.0%, respectively. Higher biofilm EPS levels and bacterial volumetric fraction within the biofilm facilitate densification and improve structural integrity, which is conducive to biofilm resistance due to limited diffusion of harmful chemicals.<sup>1,51</sup> Accordingly, bacterial live/dead ratios at the bottom layers were significantly higher than those at the surface layers for the PAE-exposed biofilms (Figure 4a). Specifically, the live/dead ratios at the surface layers were  $1.32 \pm 0.11$ ,  $1.10 \pm 0.12$ , and  $1.32 \pm 0.06$  for biofilms separately treated with 1  $\mu\text{g/L}$  DMP, 2  $\mu\text{g/L}$  DnHP, or 5  $\mu\text{g/L}$  DEHP, respectively, while the corresponding live/dead ratios at the bottom layers were  $1.63 \pm 0.06$ ,  $2.23 \pm 0.07$ , and  $2.01 \pm 0.10$ .

AFM imaging verified biofilm densification and enhanced structural stability with improved biofilm elastic modulus ( $E$ ) after PAE exposure (Figure 4b). The elastic modulus increased by 4.1-, 3.5-, and 3.0-fold relative to the unexposed biofilm when the biofilms were exposed to 1  $\mu\text{g/L}$  DMP, 2  $\mu\text{g/L}$  DnHP, or 5  $\mu\text{g/L}$  DEHP, respectively. When the biofilm was not exposed to PAEs, the very hard, hard, middle, and soft fractions of biofilm were about 1.4, 2.9, 30.4, and 65.2%, respectively. When biofilms were exposed to 1  $\mu\text{g/L}$  DMP, the hard fraction increased, with corresponding fractions making up 2.9, 21.4, 48.6, and 27.1%, respectively. Similar trends were observed for biofilms exposed to 2  $\mu\text{g/L}$  DnHP or 5  $\mu\text{g/L}$  DEHP. Improved structural stability contributes to biofilm resistance to multiple environmental stressors including disinfectants and fluid shear force.<sup>38</sup>

AFM imaging revealed that the biofilm surface became more conducive to biofilm expansion due to increased roughness after PAE exposure. The biofilm roughness increased from 24.4 to 38.4 nm, 37.3 and 29.0 nm when the biofilms were exposed to 1  $\mu\text{g/L}$  DMP, 2  $\mu\text{g/L}$  DnHP, and 5  $\mu\text{g/L}$  DEHP, respectively (Figure S5). Increased surface roughness is associated with enlarged biofilm surface area and low shear stress zones near roughness asperities, which facilitate planktonic bacteria attachment and prevent colonized bacteria dispersion by the local flow conditions.<sup>38,53</sup> Consistently, the number of planktonic bacteria was significantly lower in the PAE-exposed culture systems relative to the unexposed control group (Figure S6). The ratio of total suspended bacteria to biofilm-dwelling bacteria decreased from 33.7% in the control

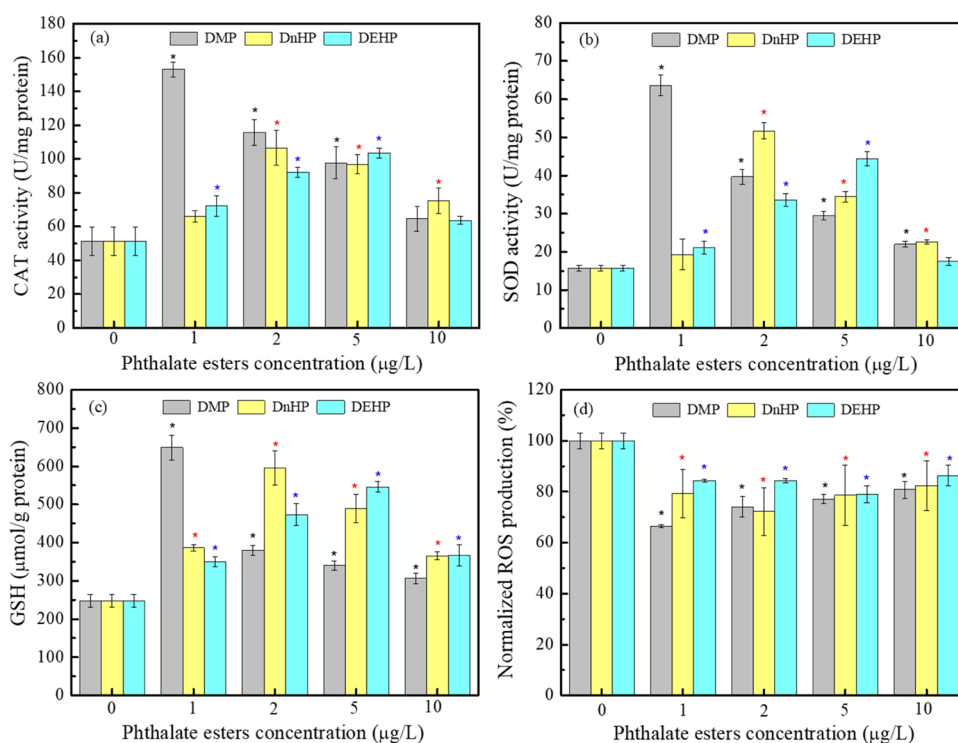


**Figure 5.** Improved antioxidative capacity within the PAE-exposed *Pseudomonas* biofilm. Upregulation of antioxidant enzymes (a, b) and nonenzymatic antioxidants (c) was associated with reduced ROS levels (d) after *Pseudomonas* biofilm exposure to different concentrations of PAEs. CAT activity, SOD activity, GSH, and ROS were determined using the CAT assay kit (visible light method), SOD assay kit (WST-1 method), GSH assay kit (microplate method), and ROS assay kit, respectively. Error bars represent  $\pm$  one standard deviation from the mean of at least independent replicates. Asterisks (\*) represent differences ( $p < 0.05$ ) between treatment and unexposed control, based on Student's *t*-test.

system to 12.3, 21.8, and 24.2% in the DMP-, DnBP-, and DEHP-exposed systems, respectively. Additionally, contact angle measurements indicate that PAE exposure increased biofilm surface hydrophobicity (Figure S7), which is associated with improved protection against chemical disinfectants via stronger repellence of water and polar disinfectants.<sup>32</sup> Higher biofilm surface hydrophobicity could also facilitate colonization of some opportunistic pathogens with hydrophobic cell surfaces such as *Mycobacterium*.<sup>54</sup>

**PAE-Stimulated Biofilm Formation Was Likely Related to Oxidative Stress.** The microbial antioxidative system includes superoxide dismutase (SOD) and catalase (CAT) as the major antioxidant enzymes and glutathione (GSH) as a nonenzymatic antioxidant.<sup>55,56</sup> Genes *msrB* and *sodM* associated with antioxidative system were upregulated by 11.2- to 11.8-fold (Figure 2), suggesting that PAEs can induce bacterial intracellular ROS (Figure S8a) and thus trigger the antioxidative system. Consistently, the SOD activity, CAT activity, and GSH concentrations increased significantly relative to the unexposed control after exposure to tested PAEs in the concentration range of 1–10 µg/L (Figure 5). For example, exposure to 1 µg/L DMP increased the SOD activity from  $15.7 \pm 0.8$  U/mg protein to  $63.6 \pm 2.8$  U/mg protein, CAT activity from  $15.7 \pm 0.8$  U/mg protein to  $63.6 \pm 2.8$  U/mg protein, and GSH concentration from  $248.2 \pm 16.6$  µmol/g protein to  $649.0 \pm 32.8$  µmol/g protein ( $p < 0.01$ ). Although not as substantial as in the case of DMP-exposed biofilm, similar upregulations of genes associated with reductase and production of SOD, CAT, and GSH were also observed for biofilms exposed to DnHP or DEHP (Figures 2 and 5). Consistent with the trends in biofilm formation and resistance

to disinfectant, 2 µg/L DnHP and 5 µg/L DEHP upregulated most associated genes and increased the SOD, CAT, and GSH levels in their individual ranges.

ROS at high concentrations are detrimental to bacteria as they can react with essential biomolecules, but ROS at lower concentrations can function in signal transduction, hormetically stimulating metabolism and therefore increasing microbial growth and thickening the biofilm.<sup>47</sup> As a result, the presence of sublethal levels of ROS-inducing agents (e.g., antibiotics and heavy metals) can stimulate biofilm formation<sup>45,46</sup> and confer biofilm enhanced resistance to multiple physical and chemical stressors.<sup>47,48</sup> Under planktonic conditions, intracellular ROS generation increased when the culture was exposed to PAEs while biofilm exposed to same levels of PAEs showed lower amounts of ROS compared with the unexposed control (Figure S8), suggesting that low levels of PAEs upregulated bacterial antioxidative systems under biofilm conditions. To test the hypothesis that the addition of PAEs increased the transient ROS generation and stimulated biofilm, a ROS scavenger (*N*-acetyl-L-cysteine with a final amount of 100 µM) was added in tandem with the PAEs to the biofilm. In the presence of the scavenger, ROS levels were similar to that of the control unexposed to PAEs and biofilm stimulation was not significant (Figure S2).

SOD catalyzes  $\cdot\text{O}_2^-$  to  $\text{O}_2$  and  $\text{H}_2\text{O}_2$ , and CAT catalyzes the dismutation of  $\text{H}_2\text{O}_2$  to water.<sup>54</sup> The n-SH group in GSH can directly react with various ROS and regenerate other cellular antioxidants.<sup>56</sup> Due to the possible overproduction of SOD, CAT, and GSH, the final ROS levels in DMP-exposed biofilm were significantly reduced by  $33.5 \pm 0.5\%$  relative to the control group (Figure 5). The high abundance of antioxidant

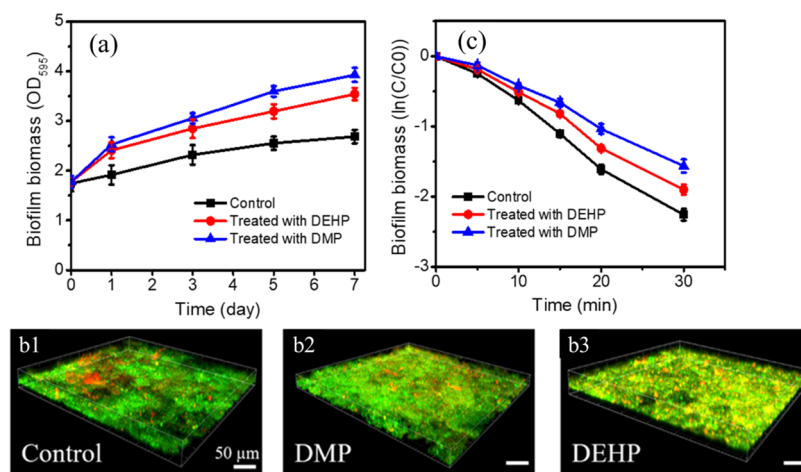


**Figure 6.** Low level of PAEs facilitate biofilm formation, densification, and disinfectant resistance. Multispecies biofilm was established on concrete coupons in standard CDC biofilm reactors. After 1-week biofilm formation, the reactors were fed with DMNB only (control), DMNB with 1  $\mu\text{g/L}$  DMP (DMP), and DMNB with 5  $\mu\text{g/L}$  DEHP (DEHP), respectively. (a) Crystal violet assay showed enhanced biofilm formation after PAE exposure. (b) CLSM imaging revealed biofilm densification after PAE exposure. (c) Sodium hypochlorite disinfection tests showed improved biofilm resistance after PAE exposure. Error bars represent  $\pm$  one standard deviation from the mean of three independent replicates.

enzymes and nonenzymatic antioxidants confers an additional capacity to mitigate the oxidative stress from disinfectant on biofilms, increasing biofilm resistance to disinfectants besides the physical barrier from biofilm densification.<sup>44,55</sup>

Incidentally, previous studies reported that hormones (e.g., estrogen) at  $\mu\text{g/L}$  levels can stimulate biofilm formation through oxidative stress.<sup>57</sup> Our results demonstrate that PAEs may similarly stimulate biofilm formation, although an etiological connection to their endocrine disruption potential seems tenuous. Moreover, although upregulation of QS genes has been reported in response to chemical stress,<sup>58</sup> further research is needed to determine whether the observed upregulation (Figure 2) was a response to PAE-related stress that is conducive to biofilm formation as a defense mechanism.

**Exposure to Low Levels of PAEs Promotes Disinfectant Resistance.** Microbes in DWDS biofilms are genotypically and phenotypically diverse.<sup>59</sup> Multispecies biofilms established in standard CDC biofilm reactors corroborated that continuous exposure to low levels of DMP (1  $\mu\text{g/L}$ ) or DEHP (5  $\mu\text{g/L}$ ) increased the biofilm biomass (Figure 6a). The overall biomass grew from  $1.7 \pm 0.2$  to  $3.9 \pm 0.2$  and  $3.4 \pm 0.3$  OD<sub>595</sub> after 1-week continuous exposure to DMP or DEHP, respectively, while the control biofilm without PAE exposure only grew to  $2.7 \pm 0.3$  OD<sub>595</sub>. The corresponding bacterial abundance was  $2.9 \pm 0.6 \times 10^9$ ,  $4.7 \pm 0.3 \times 10^9$ , and  $4.1 \pm 0.5 \times 10^9$  cells/cm<sup>2</sup> for unexposed, DMP-, and DEHP-exposed biofilms (Figure S9a), respectively. Consistent with the single species biofilm, EPS abundance increased by 53.9 and 40.6% after continuous exposure to DMP or DEHP (Figure S9b), respectively. Moreover, PAE-exposed multispecies biofilms were densified with the bacterial volumetric fraction increasing from  $0.56 \pm 0.07$  for unexposed control to  $0.74 \pm 0.04$  and  $0.68 \pm 0.05$  for DMP- and DEHP-exposed biofilm (Figures 6b and S9c). Accordingly, the PAE-exposed biofilms exhibited enhanced resistance to chlorine with bacterial decay rate at  $0.049 \pm 0.005$ ,  $0.062 \pm 0.006$ , and  $0.075 \pm 0.006$  min<sup>-1</sup> for DMP-exposed, DEHP-exposed, and unexposed control, respectively (Figure 6c).

Biofilms in municipal water distribution systems can shelter pathogens from disinfectants and provide stable environments for horizontal gene transfer. Several PAEs are regulated by

drinking water guidelines due to their potential ecotoxicity and carcinogenicity. For example, the current maximum contaminant level (MCL) set by the USEPA for DEHP is 6  $\mu\text{g/L}$ .<sup>60</sup> Although concentrations below these levels are considered safe to humans, the indirect detrimental consequences due to their effects on DWDS biofilm growth, densification, and higher resistance to disinfectants (and associated microbial risks) should not be neglected. Low PAE levels (from  $\mu\text{g/L}$  to ng/L) that commonly occur in DWDS and other environments can accumulate within biofilms because of their relatively stable chemical properties and high affinity for the biofilm matrix.<sup>21</sup> PAE-induced biofilm growth (Figure 3) and increase in biofilm surface hydrophobicity (Figure S7) may further enhance PAE absorption from bulk solution and accumulation within the biofilm. Considering also potential PAE-induced biofilm densification and upregulation of QS, this raises the possibility of a feedback loop leading to more resilient, disinfectant-resistant biofilms, which should stimulate further research on this overlooked phenomenon.

**Environmental Implications.** PAEs are ubiquitous and seem inevitable considering the sheer amount of plastic debris in natural environments and the widespread use of plastic products in engineered and agricultural systems. The possible enhancement of biofilm resiliency by low levels of PAEs may not be limited to drinking water systems given the prevalence of biofilms in industrial, medical, and environmental contexts. From the human mucosal surface to agricultural environments,<sup>61,62</sup> biofilms more resistant to antimicrobial agents imply lower efficacy of our current array of tools to eliminate problematic bacteria, which may require novel microbial control strategies. Bacterial biofilms are the dominant contributors to human infection and responsible for food contamination and the subsequent transmission of foodborne disease; more robust biofilms stimulated by low levels of PAEs may make outbreaks of foodborne disease more common and more difficult to treat.

Overall, a variety of incidentally introduced or *in situ* generated PAEs (often found in DWDS at similar concentrations as those tested in this work) can upregulate biofilm bacteria quorum sensing and affect biofilm physiology, stimulating biofilm growth and resistance to common



disinfectants. Given that biofilms are a pervasive challenge in medical, industrial, and environmental systems, the scale and significance of this overlooked phenomenon to public health and critical microbial processes (e.g., microbial induced corrosion) warrant further investigation.

## ■ ASSOCIATED CONTENT

### SI Supporting Information

The Supporting Information is available free of charge at <https://pubs.acs.org/doi/10.1021/acs.est.1c04857>.

Bacterial composition in initial and treated biofilms, biofilm of different maturity in response to phages, biofilm resistance to re-infection by high phage concentration, biofilm bacteria decay rate during disinfection with chlorine, phage growth parameters in different hosts, and detailed information on functional genes (PDF)

## ■ AUTHOR INFORMATION

### Corresponding Authors

**Pingfeng Yu** – College of Environmental and Resource Sciences, Zhejiang University, Hangzhou 310058, China; Department of Civil and Environmental Engineering, Rice University, Houston 77005, United States; [orcid.org/0000-0003-0402-773X](https://orcid.org/0000-0003-0402-773X); Email: [yupf@zju.edu.cn](mailto:yupf@zju.edu.cn)

**Pedro J. J. Alvarez** – Department of Civil and Environmental Engineering, Rice University, Houston 77005, United States; [orcid.org/0000-0002-6725-7199](https://orcid.org/0000-0002-6725-7199); Email: [alvarez@rice.edu](mailto:alvarez@rice.edu)

### Authors

**Haibo Wang** – Key Laboratory of Drinking Water Science and Technology, Research Center for Eco-Environmental Sciences, Chinese Academy of Sciences, Beijing 100085, China

**Cory Schwarz** – Department of Civil and Environmental Engineering, Rice University, Houston 77005, United States

**Bo Zhang** – School of Resources and Environment, Northeast Agricultural University, Harbin 150030, China

**Lixin Huo** – Key Laboratory of Drinking Water Science and Technology, Research Center for Eco-Environmental Sciences, Chinese Academy of Sciences, Beijing 100085, China

**Baoyou Shi** – Key Laboratory of Drinking Water Science and Technology, Research Center for Eco-Environmental Sciences, Chinese Academy of Sciences, Beijing 100085, China; [orcid.org/0000-0003-2129-4717](https://orcid.org/0000-0003-2129-4717)

Complete contact information is available at: <https://pubs.acs.org/doi/10.1021/acs.est.1c04857>

### Notes

The authors declare no competing financial interest.

## ■ ACKNOWLEDGMENTS

This work was supported by NSF ERC on Nanotechnology-Enabled Water Treatment (EEC-1449500), National Natural Science Foundation of China (51878654 and 52070189), and National Key Research and Development Program of China (2019YFD1100105). The authors thank Ruonan Sun and Alloysius J. Budi Utama for their help in biofilm characterization.

## ■ REFERENCES

- (1) Xue, Z.; Sendamangalam, V. R.; Gruden, C. L.; Seo, Y. Multiple roles of extracellular polymeric substances on resistance of biofilm and detached clusters. *Environ. Sci. Technol.* **2012**, *46*, 13212–13219.
- (2) Zhang, J.; Li, W.; Chen, J.; Wang, F.; Qi, W.; Li, Y. Impact of disinfectant on bacterial antibiotic resistance transfer between biofilm and tap water in a simulated distribution network. *Environ. Pollut.* **2019**, *246*, 131–140.
- (3) Zhang, B.; Yu, P.; Wang, Z.; Alvarez, P. J. J. Hormetic promotion of biofilm growth by polyvalent bacteriophages at low concentrations. *Environ. Sci. Technol.* **2020**, *54*, 12358–12365.
- (4) Wang, H.; Hu, C.; Zhang, L.; Li, X.; Zhang, Y.; Yang, M. Effects of microbial redox cycling of iron on cast iron pipe corrosion in drinking water distribution systems. *Water Res.* **2014**, *65*, 362–370.
- (5) Kip, N.; van Veen, J. A. The dual role of microbes in corrosion. *ISME J.* **2015**, *9*, 542–551.
- (6) Enger, K. S.; Nelson, K. L.; Clasen, T.; Rose, J. B.; Eisenberg, J. N. S. Linking quantitative microbial risk assessment and epidemiological data: informing safe drinking water trials in developing countries. *Environ. Sci. Technol.* **2012**, *46*, 5160–5167.
- (7) Liu, S.; Gunawan, C.; Barraud, N.; Rice, S. A.; Harry, E. J.; Amal, R. Understanding, monitoring, and controlling biofilm growth in drinking water distribution systems. *Environ. Sci. Technol.* **2016**, *50*, 8954–8976.
- (8) Pinto, A. J.; Xi, C.; Raskin, L. Bacterial community structure in the drinking water microbiome is governed by filtration processes. *Environ. Sci. Technol.* **2012**, *46*, 8851–8859.
- (9) Huang, X.; Andry, S.; Yaputri, J.; Kelly, D.; Ladner, D. A.; Whelton, A. J. Crude oil contamination of plastic and copper drinking water pipes. *J. Hazard. Mater.* **2017**, *339*, 385–394.
- (10) Marttinen, S. K.; Kettunen, R. H.; Sormunen, K. M.; Rintala, J. A. Removal of bis(2-ethylhexyl) phthalate at a sewage treatment plant. *Water Res.* **2003**, *37*, 1385–1393.
- (11) Skjevrak, I.; Due, A.; Gjerstad, K. O.; Herikstad, H. Volatile organic components migrating from plastic pipes (HDPE, PEX and PVC) into drinking water. *Water Res.* **2003**, *37*, 1912–1920.
- (12) Wang, Y.; Wang, F.; Xiang, L.; Gu, C.; Redmile-Gordon, M.; Sheng, H.; Wang, Z.; Fu, Y.; Bian, Y.; Jiang, X. Risk assessment of agricultural plastic films based on release kinetics of phthalate acid esters. *Environ. Sci. Technol.* **2021**, *56*, 3676–3685.
- (13) Zhan, Y.; Sun, J.; Luo, Y.; Pan, L.; Deng, X.; Wei, Z.; Zhu, L. Estimating emissions and environmental fate of di-(2-ethylhexyl) phthalate in Yangtze River delta, China: application of inverse modeling. *Environ. Sci. Technol.* **2016**, *50*, 2450–2458.
- (14) Deng, H.; Li, R.; Yan, B.; Li, B.; Chen, Q.; Hu, H.; Xu, Y.; et al. PAEs and PBDEs in plastic fragments and wetland sediments in Yangtze estuary. *J. Hazard. Mater.* **2021**, *409*, No. 124937.
- (15) Wang, L.; Gu, Y.; Zhang, Z.; Sun, A.; Shi, X.; Chen, J.; Lu, Y. Contaminant occurrence, mobility and ecological risk assessment of phthalate esters in the sediment-water system of the Hangzhou Bay. *Sci. Total Environ.* **2021**, *770*, No. 144705.
- (16) Domínguez-Moruco, N.; Gonzalez-Alonso, S.; Valcarcel, Y. Phthalate occurrence in rivers and tap water from central Spain. *Sci. Total Environ.* **2014**, *500-501*, 139–146.
- (17) Liu, X.; Shi, J.; Bo, T.; Li, H.; Crittenden, J. C. Occurrence and risk assessment of selected phthalates in drinking water from waterworks in China. *Environ. Sci. Pollut. Res.* **2015**, *22*, 10690–10698.
- (18) Shin, H. M.; Dhar, U.; Calafat, A. M.; Nguyen, V.; Schmidt, R. J.; Hertz-Picciotto, I. Temporal trends of exposure to phthalates and phthalate alternatives in California pregnant women during 2007–2013: comparison with other populations. *Environ. Sci. Technol.* **2020**, *54*, 13157–13166.
- (19) Gunaalan, K.; Fabbri, E.; Capolupo, M. The hidden threat of plastic leachates: a critical review on their impacts on aquatic organisms. *Water Res.* **2020**, *184*, No. 116170.
- (20) Zhang, Y.; Jiao, Y.; Li, Z.; Tao, Y.; Yang, Y. Hazards of phthalates (PAEs) exposure: a review of aquatic animal toxicology studies. *Sci. Total Environ.* **2021**, *771*, No. 145418.



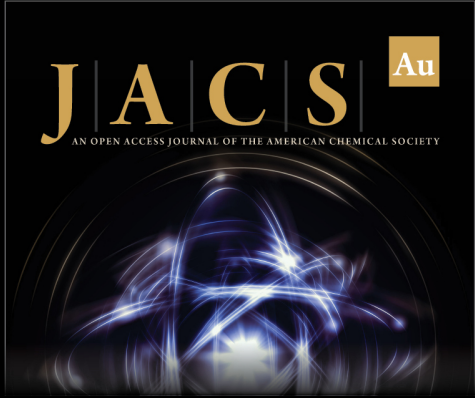
- (21) Wang, Z.; Wang, C.; You, Y.; Xu, W.; Lv, Z.; Liu, Z.; Chen, W.; Shi, Y.; Wang, J. Response of *Pseudomonas fluorescens* to dimethyl phthalate. *Ecotoxicol. Environ. Saf.* **2019**, *167*, 36–43.
- (22) You, Y.; Wang, Z.; Xu, W.; Wang, C.; Zhao, X.; Su, Y. Phthalic acid esters disturbed the genetic information processing and improved the carbon metabolism in black soils. *Sci. Total Environ.* **2019**, *653*, 212–222.
- (23) Li, Y.; Zhang, P.; Wang, L.; Wang, C.; Zhang, W.; Zhang, H.; Niu, L.; Wang, P.; Cai, M.; Li, W. Microstructure, bacterial community and metabolic prediction of multi-species biofilms following exposure to di-(2-ethylhexyl phthalate) (DEHP). *Chemosphere* **2019**, *237*, No. 124382.
- (24) Amaral-Zettler, L. A.; Zettler, E. R.; Mincer, T. J. Ecology of the plastisphere. *Nat. Rev. Microbiol.* **2020**, *18*, 139–151.
- (25) Paluselli, A.; Faucelle, V.; Galgani, F.; Sempere, R. Phthalate release from plastic fragments and degradation seawater. *Environ. Sci. Technol.* **2019**, *53*, 166–173.
- (26) Ye, J.; Zhang, K.; Yuan, X.; J, H.; Hu, M.; Huang, T.; Ge, R. Di-n-hexyl phthalate causes Leydig cell hyperplasia in rats during puberty. *Toxicol. Lett.* **2020**, *332*, 213–221.
- (27) Le, T. M.; Nguyen, H. M. N.; Nguyen, V. K.; Nguyen, A. V.; Vu, N. D.; Yen, N. T. H.; Hoang, A. Q.; Minh, T. B.; Kannan, K.; Tran, T. M. Profiles of phthalic acid esters (PAEs) in bottled water, tap water, lake water, and wastewater samples collected from Hanoi, Vietnam. *Sci. Total Environ.* **2021**, *788*, No. 147831.
- (28) Liu, Y.; Li, J. Role of *Pseudomonas aeruginosa* biofilm in the initial adhesion, growth and detachment of *Escherichia coli* in porous meida. *Environ. Sci. Technol.* **2008**, *42*, 443–449.
- (29) Whiteley, M.; Bangera, M. G.; Bumgarner, R. E.; Parsek, M. R.; Teitzel, G. M.; Lory, S. L.; Greenberg, E. P. Gene expression in *Pseudomonas aeruginosa* biofilms. *Nature* **2001**, *413*, 860–864.
- (30) Mena, K. D.; Gerba, C. P. Risk assessment of *Pseudomonas aeruginosa* in water. *Rev. Environ. Contam. Toxicol.* **2009**, *201*, 71–115.
- (31) Yu, P.; Mathieu, J.; Yang, Y.; Alvarez, P. J. J. Suppression of enteric bacteria by bacteriophages: importance of phage polyvalence in the presence of soil bacteria. *Environ. Sci. Technol.* **2017**, *51*, 5270–5278.
- (32) Epstein, A. K.; Pokroy, B.; Seminara, A.; Aizenberg, J. Bacterial biofilm shows persistent resistance to liquid wetting and gas penetration. *Proc. Natl. Acad. Sci. USA.* **2011**, *108*, 995–1000.
- (33) Yang, G.; Lin, J.; Zeng, E. Y.; Zhuang, L. Extraction and characterization of stratified extracellular polymeric substances in *Geobacter* biofilms. *Bioresour. Technol.* **2019**, *276*, 119–126.
- (34) Liu, G.; Bakker, G. L.; Li, S.; Vreeburg, J. H. G.; Verberk, J. Q. J. C.; Medema, G. J.; Liu, W. T.; Dijk, J. C. Pyrosequencing reveals bacterial communities in unchlorinated drinking water distribution system: an integral study of bulk water, suspended solids, loose deposits, and pipe wall biofilm. *Environ. Sci. Technol.* **2014**, *48*, 5467–5476.
- (35) Yu, P.; Wang, Z.; Marcos-Hernandez, M.; Zuo, P.; Zhang, D.; Powell, C.; Pan, A. Y.; Villagran, D.; Wong, M. S.; Alvarez, P. J. J. Bottom-up biofilm eradication using bacteriophage-loaded magnetic nanocomposites: a computational and experimental study. *Environ. Sci.: Nano* **2019**, *6*, 3539–3550.
- (36) Qu, C.; Qian, S.; Chen, L.; Guan, Y.; Zheng, L.; Liu, S.; Chen, W.; Cai, P.; Huang, Q. Size-dependent bacterial toxicity of hematite particles. *Environ. Sci. Technol.* **2019**, *53*, 8147–8156.
- (37) Oh, Y. J.; Lee, N. R.; Jo, W.; Jung, W. K.; Lim, J. S. Effects of substrates on biofilm formation observed by atomic force microscopy. *Ultramicroscopy* **2009**, *109*, 874–880.
- (38) Shen, Y.; Huang, C.; Monroy, G. L.; Janjaroen, D.; Derlon, N.; Lin, J.; Espinosa-Marzal, R.; Morgenroth, E.; Boppart, S. A.; Ashbolt, N. J.; Liu, W. T.; Nguyen, T. H. Response of simulated drinking water biofilm mechanical and structural properties to long-term disinfectant exposure. *Environ. Sci. Technol.* **2016**, *50*, 1779–1787.
- (39) Suriano, R.; Credi, C.; Levi, M.; Turri, S. AFM nanoscale indentation in air of polymeric and hybrid materials with highly different stiffness. *Appl. Surf. Sci.* **2014**, *311*, 558–566.
- (40) Pickering, H.; Wu, M.; Bradley, M.; Bridle, H. Analysis of *Giardia lamblia* interactions with polymer surfaces using a microarray approach. *Environ. Sci. Technol.* **2012**, *46*, 2179–2186.
- (41) Liu, B. H.; Yu, L. C. In-situ, time-lapse study of extracellular polymeric substance discharge in *Streptococcus mutans* biofilm. *Colloids Surf., B* **2017**, *150*, 98–105.
- (42) Wang, Y.; Lu, J.; Zhang, S.; Li, J.; Mao, L.; Yuan, Z.; Bond, P.; Guo, J. Non-antibiotic pharmaceuticals promote the transmission of multidrug resistance plasmids through intra-and intergenera conjugation. *ISME J.* **2021**, *15*, 2493–2508.
- (43) Yang, Y.; Alvarez, P. J. J. Sublethal concentrations of silver nanoparticles stimulate biofilm development. *Environ. Sci. Technol. Lett.* **2015**, *2*, 221–226.
- (44) Romsang, A.; Atichartpongkul, S.; Trinachartvanit, W.; Vattanaviboon, P.; Mongkolsuk, S. Gene expression and physiological role of *Pseudomonas aeruginosa* methionine sulfoxide reductases during oxidative stress. *J. Bacteriol.* **2013**, *195*, 3299–3308.
- (45) Wang, H.; Shen, Y.; Hu, C.; Xing, X.; Zhao, D. Sulfadiazine/ciprofloxacin promote opportunistic pathogens occurrence in bulk water of drinking water distribution systems. *Environ. Pollut.* **2018**, *234*, 71–78.
- (46) Yang, Y.; Mathieu, J. M.; Chattopadhyay, S.; Miller, J. T.; Wu, T.; Shibata, T.; Guo, W.; Alvarez, P. J. J. Defense mechanisms of *Pseudomonas aeruginosa* PAO1 against quantum dots and their released heavy metals. *ACS Nano* **2012**, *6*, 6091–6098.
- (47) Gambino, M.; Cappitelli, F. Mini-review: biofilm response to oxidative stress. *Biofouling* **2016**, *32*, 167–178.
- (48) Pezzoni, M.; Pizarro, R. A.; Costa, C. S. Exposure to low doses of UVA increases biofilm formation in *Pseudomonas aeruginosa*. *Biofouling* **2018**, *34*, 673–684.
- (49) Ahimou, F.; Semmens, M. J.; Haugstad, G.; Novak, P. J. Effect of protein, polysaccharide, and oxygen concentration profiles on biofilm cohesiveness. *Appl. Environ. Microbiol.* **2007**, *73*, 2905–2910.
- (50) Hall, C. W.; Mah, T. F. Molecular mechanisms of biofilm-based antibiotic resistance and tolerance in pathogenic bacteria. *FEMS Microbiol. Rev.* **2017**, *41*, 276–301.
- (51) Xue, Z.; Lee, W. H.; Coburn, K. M.; Seo, Y. Selective reactivity of monochloramine with extracellular matrix components affects the disinfection of biofilm and detached clusters. *Environ. Sci. Technol.* **2014**, *48*, 3832–3839.
- (52) Coburn, K. M.; Wang, Q.; Rediske, D.; Viola, R. E.; Hanson, B. L.; Xue, Z.; Seo, Y. Effects of extracellular polymeric substance composition on bacteria disinfection by monochloramine: application of MALDI-TOF/TOF-MS and multivariate analysis. *Environ. Sci. Technol.* **2016**, *50*, 9197–9205.
- (53) Shen, Y.; Monroy, G. L.; Derlon, N.; Janjaroen, D.; Huang, C.; Morgenroth, E.; Boppart, S. A.; Ashbolt, N. J.; Liu, W. T.; Nguyen, T. H. Role of biofilm roughness and hydrodynamic conditions in *Legionella pneumophila* adhesion to and detachment from simulated drinking water biofilms. *Environ. Sci. Technol.* **2015**, *49*, 4274–4282.
- (54) Bansal-Mutalik, R.; Nikaido, H. Mycobacterial outer membrane is a lipid bilayer and the inner membrane is unusually rich in diacyl phosphatidylinositol dimannosides. *Proc. Natl. Acad. Sci. U.S.A.* **2014**, *111*, 4958–4963.
- (55) Wang, W.; Wang, H.; Li, G.; An, T.; Zhao, H.; Wong, P. K. Catalyst-free activation of persulfate by visible light for water disinfection: efficiency and mechanisms. *Water Res.* **2019**, *157*, 106–118.
- (56) Li, S.; Chi, Z.; Li, W. In vitro toxicity of dimethyl phthalate to human erythrocytes: from the aspects of antioxidant and immune functions. *Environ. Pollut.* **2019**, *253*, 239–245.
- (57) Chotirmall, S. H.; Smith, S. G.; Gunaratnam, C.; Cosgrove, S.; Dimitrov, B. D.; O'Neill, S. J.; Harvey, B. J.; Greene, C. M.; McElvaney, N. G. Effect of estrogen on *Pseudomonas mucoidy* and exacerbations in cystic fibrosis. *N. Engl. J. Med.* **2012**, *366*, 1978–1986.
- (58) Bruger, E. L.; Snyder, D.; Cooper, V. S.; Waters, C. M. Quorum sensing provides a molecular mechanism for evolution to tune and maintain investment in cooperation. *ISME J.* **2021**, *15*, 1236–1247.

(59) Hull, N. M.; Ling, F.; Pinto, A. J.; Albertsen, M.; Jang, H. G.; Hong, P. Y.; Konstantinidis, K. T.; LeChevallier, M.; Colwell, R. R.; Liu, W. T. Drinking water microbiome project: is it time? *Trends Microbiol.* **2019**, *27*, 670–677.


(60) USEPA. *National Primary Drinking Water Regulations*; United States Environ. Prot. Agency, 2009.


(61) Zhang, H.; DiBaise, J. K.; Zuccolo, A.; Kudrna, D.; Braidotti, M.; Yu, Y.; Parameswaran, P.; Crowell, M. D.; Wing, R.; Rittmann, B. E.; Krajmalnik-Brown, R. Human gut microbiota in obesity and after gastric bypass. *Proc. Natl. Acad. Sci. U.S.A.* **2009**, *106*, 2365–2370.


(62) De Cesare, F.; Mattia, E. D.; Zussman, E.; Macagnano, A. A 3D soil-like nanostructured fabric for the development of bacterial biofilms for agricultural and environmental uses. *Environ. Sci.: Nano* **2020**, *7*, 2546–2572.



**JACS Au**  
AN OPEN ACCESS JOURNAL OF THE AMERICAN CHEMICAL SOCIETY

 Editor-in-Chief  
**Prof. Christopher W. Jones**  
Georgia Institute of Technology, USA

**Open for Submissions** 

pubs.acs.org/jacsau  ACS Publications  
Most Trusted. Most Cited. Most Read.